

Discerning the success of sustainable planning: A comparative analysis of urban heat island dynamics in Korean new towns



Yoonshin Kwak^a, Chan Park^{b,*}, Brian Deal^a

^a Department of Landscape Architecture, University of Illinois at Urbana-Champaign, USA

^b Department of Landscape Architecture, University of Seoul, Republic of Korea

ARTICLE INFO

Keywords:

Surface urban heat islands (SUHI)
Land surface temperatures (LST)
Korean new towns
Remote sensing
K-mean clustering
Sustainable planning

ABSTRACT

UHI is an important measure for understanding the urban landscape, especially in terms of thermal agglomeration and disturbance. This research aims to discern the success of sustainability planning by examining and comparing the different characteristics of UHIs through the combination of machine learning and statistical methods. To achieve this, we analyze 4 new towns in Korea, which include two 'old' new towns and two 'recent' new towns. The key difference between our test towns lies on whether or not the sustainability policies were applied to their development plans. We visualize LST and conduct a *k*-mean clustering to find and quantify spatial patterning in the resulting UHI measures. We then compare the statistical relations between LST and 6 UHI driven variables across the towns. Using comparative analysis, this research reveals that sustainable development policies have a notable effect on the patterns and intensities of UHI. Urban structures, planned under development policies, including green and blue space ratios, road networks, and housing distributions, were found to affect UHI significantly. We quantifiably confirm that the sustainability policies implemented in planning the 'recent' new towns allow the towns to experience less aggravated UHIs than the 'old' new towns. However, we also claim a need to develop appropriate, long-term UHI management regulations for the 'recent' new towns. This paper provides a solid basis for improving Korean new town planning and managing the environmental issues in urban systems for planners, designers, and decision-makers to establish the sustainable built environment.

1. Introduction

Sustainability in urban development has gained international attention at a time when cities across the world are confronting a wide array of unintended consequences from anthropogenic activities (Golden, 2004; Rasoolimanesh, Badarulzaman, & Jaafar, 2011). Current projections show that such consequences are being exacerbated by an incremental increase in urban population (Grimm et al., 2008; United Nations, 2018). These increasing population trends have accelerated the intensive conversion of natural land to built-up, urbanized lands that have exponentially more mass and less perviousness (Xu, 2010). As a result, urban areas produce much higher temperatures than surrounding areas. This phenomenon, called the urban heat island (UHI), is considered one of the most challenging issues that currently impinge on the overall sustainability of our cities (Grimm et al., 2008; Pickard, Van Berkel, Petrasova, & Meentemeyer, 2017; Voogt & Oke, 2003).

UHI is an important measure for understanding the urban sustainability. Especially, highlighting the Goal 11 of the United Nation's SDGs

(Sustainable Development Goals) –“Make cities and human settlements inclusive, safe, resilient and sustainable,” UHI is one of good indicators of public health (Heaviside, Vardoulakis, & Cai, 2016) and energy efficiency (Arifwidodo & Chandrasiri, 2015). In terms of thermal agglomeration and disturbance (Mahlkow & Donner, 2017), a high UHI measurement can signal significant human-induced impacts on the landscape (Zhao, Lee, Smith, & Oleson, 2014). Examining and comparing the underlying mechanisms of UHI can be used to estimate an area's energy balance among other useful growth-related insights. For example, Keeratikasikorn, Bonafoni, Keeratikasikorn, and Bonafoni (2018) use UHI measures to address the importance of lowering built-up density and reducing the thermal impacts of rapid growth patterns in a study of six major cities in Thailand. Estoque, Murayama, and Myint (2017) use UHI measures to exemplify the relationship between land surface temperature (LST) and green space distribution in a study of three megacities in South Asia. The literature on UHI (see Clinton & Gong, 2013) suggests that UHIs are fundamentally a product of development intensity, vegetation, and urban extent (Ju, Dronova, Ma, &

* Corresponding author.

E-mail addresses: yk23@illinois.edu (Y. Kwak), chaneparkmomo7@uos.ac.kr (C. Park), deal@illinois.edu (B. Deal).

<https://doi.org/10.1016/j.scs.2020.102341>

Received 6 January 2020; Received in revised form 12 June 2020; Accepted 13 June 2020

Available online 16 June 2020

2210-6707/ © 2020 Elsevier Ltd. All rights reserved.

Zhang, 2017; Li et al., 2018; Tran, Uchihama, Ochi, & Yasuoka, 2006; Zhou, Zhao, Liu, Zhang, & Zhu, 2014).

The urban thermal environment is a result of a set of accumulated and ongoing anthropogenic activities, giving every city a distinct thermal pattern dynamic and a unique UHI measure (Peng, Xie, Liu, & Ma, 2016). Previous studies have shown that UHIs are context-dependent relating to urban forms, surface conditions, climate and topography (Connors, Galletti, & Chow, 2013; Estoque et al., 2017; Keeratikasikorn et al., 2018), and considerable evidence has proved that urbanization – changes in land-uses, have a profound impact on the thermal environment (Mathew, Khandelwal, & Kaul, 2016). The magnitude of UHIs reflects the ways in which cities respond to or manage urban growth. However, there are discrepancies between the findings in literature across cities, regions, and time scales (Yin, Yuan, Lu, Huang, & Liu, 2018), and we know little of the complex interplays between UHI and different physical processes of urban growth (Cui, Xu, Dong, & Qin, 2016). Moreover, little attention has been paid to using the various context-dependent UHIs for the evaluation of development policies. Understanding this would help decision-makers, planners, and researchers manage the urban environment more sustainably.

This study emphasizes the usefulness of evaluating UHI as a parameter to test the success of sustainable development strategies. We use UHI to evaluate the sustainability of planning policies incorporated in the development of 4 Korean new towns. We choose to stay in one region so that we can reliably keep several sociocultural and environmental factors constant in our natural (comparative) experiment. We assume for example, that the towns share the same climate conditions - each is located within 20 km of Seoul; each shares the same sociocultural pressures; and each shares the same market and other economic forcings. Our study sites include two 'old' new towns, completely built-out in the middle of the 1990s, and two 'recent' new towns where the construction was launched in the middle of the 2000s and are just completing build-out. The key difference between our test sites lies on whether or not the concept of sustainability was applied to their development plans. In the 'old' new towns, concepts of sustainability were not considered, while the 'recent' new towns were planned using sustainability principles. We argue this difference should have a notable impact on the urban form (including population density, green space ratio, and road network structures) and their subsequent UHI measures.

The hypotheses of this research can be summarized twofold. First, we hypothesize that thermal dynamic can be measured to delineate the spatiotemporal patterns and intensities of urbanization over time. To test this, we visualize LST to represent the years from 2002 to 2017 and conduct a cluster analysis to find spatial patterning in the resulting UHI measures. The findings from the first hypothesis visually represent the difference in UHIs between the 'old' new towns and 'recent' new towns, leading to our second hypothesis that explores 'how.' The second hypothesis is that our UHI measure significantly reflect the effect of sustainable development policies applied to the city development. We examine this hypothesis by analyzing the statistical relations and comparing the differences between test cases.

In the following, we review the existing literature to discuss technical advances in capturing UHI and its underlying mechanisms of influence (Section 2). We then introduce the detailed context of our four study areas with a focus on their developmental processes and their differences that we hypothesize will affect the patterns of UHI (Section 3). In Section 4, we discuss some of the methodologies used in our UHI comparative analysis including: *k*-mean clustering, data retrieval processes, and regression analyses. We present the results of our analysis in Section 5 with a discussion of their implications in Section 6. Section 7 concludes with some summary remarks on the major findings, the limitations of the work, and some recommended future research.

2. Literature review

2.1. Atmospheric UHI and surface UHI

Owing to the technological advancements in data capture and analysis, the extant studies in UHI have contributed to extensive variations in its definition, measurements, and assessment (Voelkel & Shandas, 2017). Studies on UHI are typically classified into two categories: atmospheric UHI (AUHI) and surface UHI (SUHI) (U.S. EPA, 2008). Studies on AUHI require direct measurements of air temperature in the canopy layer, which consists of the ground-based collection either at the meteorological stations or by automobile transects (Sagris & Sepp, 2017; Tran et al., 2006). Voelkel and Shandas (2017) noted that ground-based methods to diagnose AUHI offer advantages that allow capturing temperatures with a high level of accuracy. In their empirical study, they conducted 'vehicular-based traverses' measurement by using temperature sensors mounted on the automobile roof in order to record the atmospheric temperature in Portland, Oregon. Kolokotroni and Giridharan (2008) also used data loggers to collect hourly based data. They investigated the potential physical characteristics of air temperature and found that surface albedo is the most important variable in determining the AUHI effect. As such, studies on AUHI typically address highly accurate data and statistics (Bozorgi, Nejadkoorki, & Mousavi, 2018). However, Erell and Williamson (2006) and Tran et al. (2006) pointed out that the major challenges of AUHI research are that the atmospheric data are normally limited to parameters monitored at measurement stations and have a poor spatial resolution. Also, expert techniques are often required in order to measure data with devices, which could be costly and time-consuming (Kindu, Schneider, Teketay, & Knoke, 2013).

Conversely, studies on SUHI are basically conducted with remote sensing technology, which has important advantages over the ground-based methods. It allows researchers to easily acquire continuous data of LST for virtually every urban and rural area on the planet at a reasonably low cost (Connors et al., 2013; Estoque et al., 2017; Voelkel & Shandas, 2017; Zhou et al., 2014). Remotely sensed data can also explicitly reveal spatial characteristics and temporal changes at multiple scales in a consistent way. The advantages of utilizing the satellite imagery have helped shape abundant research on SUHI, gaining a lot of attention in the scientific community (Bozorgi et al., 2018; Imhoff, Zhang, Wolfe, & Bounoua, 2010; Kindu et al., 2013; Sagris & Sepp, 2017). This research investigates spatial and temporal UHI effects and will therefore focus on SUHI using remote sensing data.

2.2. Planning implications of UHI studies

The key advantages of remote sensing data have led to a discussion of diverse approaches for investigating the UHI phenomenon in support of sustainable urban planning. For example, much of UHI research has illustrated spatiotemporal variance of the phenomenon at multiple scales (Coutts, Beringer, & Tapper, 2007; Mathew et al., 2016), examined relations between LST and a variety of urban and environmental factors (Bokaie, Zarkesh, Arasteh, & Hosseini, 2016; Khandelwal, Goyal, Kaul, & Mathew, 2018; Tran et al., 2006), and attempted to identify the most determinant factors of the increase in LST (Imhoff et al., 2010; Zhao et al., 2014; Zhou et al., 2014). Li et al. (2018)b quantified the highly positive relation between LST and impervious surface areas concerning the linear functions of LST. Connors et al. (2013) similarly examined the relations between surface temperature and land-use patterns, also demonstrating that the impacts are context-dependent and differ across the land-uses. Peng et al. (2016) studied the effects of landscape proportions on LST in Beijing. They found the proportion of ecological land had the most significant relationship to LST and revealed that a cooling effect became pronounced when the proportion reached 70 % of the total area of the city.

There has been a specific emphasis on statistical regression methods

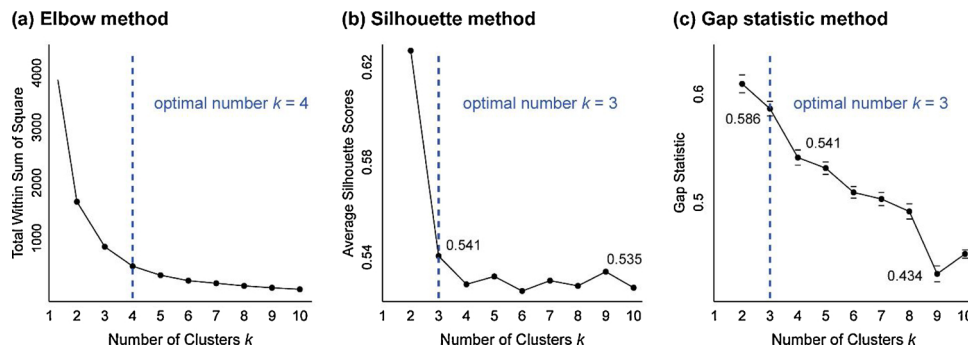


Fig. 2. Determination of the Optimal Number of the Clusters. (a) Elbow method, (b) Silhouette method, and (c) Gap statistic method.

summarizes noteworthy environmental and sociocultural characteristics of the study areas.

Despite characteristic differences, the four study areas share a similar developmental process –dramatic changes in land-use in a short period of time (i.e., they were all built out quickly). They are all also mostly urbanized and located within 20 km of Seoul with similar atmospheric characteristics and sociocultural characteristics. In the following sections, we compare the thermal environments of the towns for a 15-year period (2002–2017), including the years when the construction began in Gwanggyo and Songdo.

4. Methodology

This study used Landsat 5 Thermal Mapper (TM), Landsat 7 Enhanced Thematic Mapper Plus (ETM+), and Landsat 8 Operational Land Imager and Thermal Infrared Sensor (OLI/TIRS) to visualize LST over the study areas for the years 2002, 2006, 2009, 2013 and 2017. The multistage Landsat images were obtained from the USGS (<https://landsat.usgs.gov>), which has corrected the radiometric and geometrical distortions before delivery (Weng, Lu, & Schubring, 2004). We first filtered images of which the cloud coverage was less than 20 percent and manually selected ones where no cloud appeared over the study areas. For each study year and city, a maximum number of available cloud-free images, at least more than two, were collected (see <http://learn.illinois.edu/UHI/SUPPLEMENTARY.html> for Landsat data sources). The images were averaged to represent the yearly temperature signature minimizing influential climate backgrounds such as humidity, rainfall, wind circulation, and solar irradiation. The images used in this study were acquired in the late morning (11 a.m. to noon) from early-June to mid-September, in which the average temperature approximately ranged from 24°C to 32°C (KMA, 2018). In selecting the images, we took into account the fact that the UHI phenomenon becomes pronounced in warm seasons when the thermal infrared sensors best detect the thermal environment (Founda & Santamouris, 2017; Shahraiyini et al., 2016). Data scarcity required using inconsistent months in our seasonal range; therefore, the selection of the images is appropriate, although not optimal. LST images were retrieved following well documented, standard procedures (Mehrotra, Bardhan, & Ramaritham, 2018; Sheng, Tang, You, Gu, & Hu, 2017; Weng et al., 2004).

4.1. Determining the optimal number of urban clusters

This study utilizes a k -means clustering approach to describe urban thermal dynamics by classifying LST data into a specified number (k) of clusters. This is one of the most widely used unsupervised classification algorithms in remote sensing (Esche, Franklin, & Wulder, 2002). It is important to investigate how the impacts of urbanization on LST are characterized over the period of development for understanding the effects of sustainable planning. In this analysis, we assume that thermal clusters represent particular levels of urbanization. More specifically, if a cluster exhibits the most dramatic change in LST over time, it should

represent an area where the most aggressive urbanization or anthropogenic activities have occurred (i.e., increases in the impervious surface ratio) (Feng, Zhao, Chen, & Wu, 2014; Mathew et al., 2016). In this regard, we expect Songdo, where most of the lands were reclaimed from the sea during the study period, to have clusters with the most drastic increases.

We use the year 2017 dataset to identify levels of urbanization for each of the study areas. 2017 is used because the urbanization process in the ‘recent’ new town category is complete by that point in time, allowing UHI cluster dynamics to correspond to the current (or most recent) urbanization intensities. Four LST images (June 15, June 22, August 26, and September 3 – all in 2017) covering all study areas were averaged (to reduce climate effects) and standardized (to reduce scaling effects) (Wang, Azzari, & Lobell, 2019). Final data images for each site were subjected to our k -means clustering process.

There is no consensus in the literature for obtaining the optimal number (k) of clusters. We therefore applied and tested the three most widely-used methods in data mining: (1) the elbow method, (2) the average silhouette method (Rousseeuw, 1987), and (3) the gap statistic methods (Tibshirani, Walther, & Hastie, 2001). Each method has drawbacks and will typically compute a different result (Wang, Abrams, Kornblau, & Coombes, 2018; Zhou, Xu, & Liu, 2017). In this analysis, the elbow method resulted in four clusters, the silhouette method suggested three, and the gap statistic method also resulted in three. Using observations described in Fig. 2, we use three as the optimal number (k) of clusters.

4.2. Validation of the clustered urban areas

In order to validate our clustering results, we examined the frequency of impervious surfaces in each cluster. Impervious surfaces have routinely been used as an urbanization indicator (Eigenbrod et al., 2011; Ju et al., 2017; Mathew, Khandelwal, & Kaul, 2018). Impervious surfaces for both Bundang and Ilsan were obtained from the Environmental Geographic Information Service (<https://egis.me.go.kr/>). For Songdo and Gwanggyo where usable data was lacking for some parts of the cities (they were under construction in 2017), we used Landsat images and classified each 30 m cell by perviousness; pervious (e.g., forest, water, and parks) or impervious (e.g., road, building, parking), applying a supervised maximum likelihood classification system (Strahler, 1980). We used the new perviousness dataset (assigning 1 to impervious and 0 to pervious) to calculate the frequency of impervious surfaces for each cluster. If our clustering is valid, in each cluster the frequency of imperviousness should correspond to a specific level of urbanization.

4.3. Urban factors and relationships

Our second hypothesis is that the UHI for each study area will be characteristically different due to the implementation (or lack thereof) of sustainable development policies. We test this by first identifying 6

UHI driven variables that describe UHI characteristics. We divide these variables by their landscape characteristics and their sociocultural characteristics.

4.3.1. Landscape variables

Three landscape variables: the Green Normalized Difference Vegetation Index (GNDVI), the Modified Normalized Difference Water Index (MNDWI), and Digital Elevation Model (DEM) represent the various landscape influences (vegetation, water, and solar aspect) on urban land surface temperatures (Estoque et al., 2017; Tran et al., 2006; Weng et al., 2004). GNDVI is a modified version of the Normalized Difference Vegetation Index (Voelkel & Shandas, 2017) that is more sensitive to low chlorophyll contents (Gitelson, Kaufman, & Merzlyak, 1996) – needed for this study because we investigate relatively small urban areas. Similarly, MNDWI detects the presence of open water but reduces built-up noises (McFeeters, 1996) and is useful for revealing the subtle variation of water bodies in urban settings (Xu, 2006). This is especially important in Songdo and Gwanggyo. In this study, we used only positive values of GNDVI and MNDWI. The relationship between elevation (DEM) and LST is well documented in the literature (Khandelwal et al., 2018; Mathew et al., 2018; Phan et al., 2018). Elevation data were acquired from the Korean National Geographic Information Institute (<http://map.ngii.go.kr/>).

4.3.2. Sociocultural variables

The Normalize Difference Built Index (NDBI), Euclidean distance to roads (EDR), and population density (PD) are used to explain the variation of LST due to sociocultural influences. NDBI is a widely-used biophysical parameter used to analyze the distribution of impervious surfaces (Bozorgi et al., 2018; Zha, Gao, & Ni, 2003). EDR represents road networks and proximity to roads, a good indicator of urbanization densities (Zhu, Wong, Guilbert, & Chan, 2017). We obtained road data from Korean Intelligent Transportation Systems (<https://nodelink.its.go.kr/>). Population data from Statistics Korea (<https://sgis.kostat.go.kr/>) help reveal relative densities (Bokaie et al., 2016).

The above 6 factors help identify the spatial characteristics of UHI across the study areas. Table 2 summarizes the 6 variables, providing a brief description and the relationship of each to UHI measurement. Spatial data is collected in 30 m × 30 m raster-based formats. Numeric values contained in corresponding cells were used to conduct multiple regression analyses for each town. Explanatory variables were normalized (0–1) to enable comparison, then sorted and broken into 70 equal-sized quantiles (see Pan, Deal, Chen, & Hewings, 2018). We calculated the expected temperature (LST) of the corresponding cells for each quantile and fitted the best model (linear or polynomial functions) based on Akaike information criterion (AIC).

5. Results

To understand the thermal dynamics of our study areas, we first

Table 2
Six urban factors selected in this study.

Category	Parameter (abbreviation)	Description / UHI connection
Landscape	GNDVI - Green Normalized Difference Vegetation Index	The presence or absence of vegetation Describes vegetative influences
	MNDWI - Modified Normalized Difference Water Index	The presence or absence of open water Describes water-based influences
	DEM - Elevation	The digital elevation model Elevation and aspect influences
Socio-culture	NDBI - Normalize Difference Built Index	The distribution of built-up areas Describes urbanization extents
	EDR - Euclidean Distance to Road	Roads and distance from roads Describes urbanization densities
	PD - Population Density	Population data in 1000 residents per unit area

visualized the spatiotemporal distributions of LST for each test site over the study years from 2002 to 2017. Each LST image was normalized between 0–1 to enable a comparison between the years and sites (Fig. 3). One notable outcome is the temporal changes in the thermal environments in both Songdo and Gwanggyo that generally reflect their developmental processes. In Songdo, a markedly high LST area can be seen at the area center (in red) surrounded by lower temperature areas (in blue) of water. This is a product of the land reclamation process (and fill) that was just in progress in 2002. The highly concentrated LST seems to begin spreading out to the entire city from the year 2006. This spreading-out represents the developmental building construction process where reclaimed lands were expanded, and the residential, industrial and commercial land-uses were introduced. In 2017 two additional high LST areas appear at the northern and southern sections of the area, marking major urban development projects (the Incheon New Port to the north; and the Incheon Global Campus to the south). In Gwanggyo a similar LST temporal pattern emerges over the study period. High LST areas appear in the central and southern parts of the town in both the 2002 and 2006 images. Considering that most of the areas remained undeveloped before and around 2006, the spots most likely represent the existing urban areas and thermal spillovers from neighboring cities. 2009 images describe high LST areas that largely prevail over the entire town at a time when most of the area was under construction. In 2009, two lakes in the southern area also become distinctive, which arguably illustrates that the town was becoming more intensively urbanized from that period in time. 2013 and 2017 images reveal a more endemic urbanization pattern, as the town features an assembling pattern of high LST at the center and northern parts. In contrast, Bundang and Ilsan were mature urban areas by 2002 (construction was completed in the middle of the 1990s) and not unexpectedly, little change takes place over the period.

5.1. Thermal dynamics

In this study, we hypothesize that analyzing thermal dynamics will help describe how intensively urban activities have evolved over a specified space and time period. Clustering enables quantification of UHI dynamics by geographies that are easier to ground truth. It also enables visualization techniques that can more readily describe the spatiotemporal changes numerically. Clustered quantitative data enables comparison between both clusters and study areas. This helps shape a more intuitive understanding to what extent urbanization processes affect thermal environments during the study period in each case.

Fig. 4 visualizes the clustering result with the optimal number of three, computed from the 20 % randomly sampled 2017 data. Cluster 3 shows the highest LST on average, followed by Cluster 2. Cluster 1 represents the areas with the lowest mean LST, and the areas of Cluster 1 account for the lowest proportion for all study areas (Table 3). It is a noteworthy finding that the proportion of Cluster 1 in the 'old' new

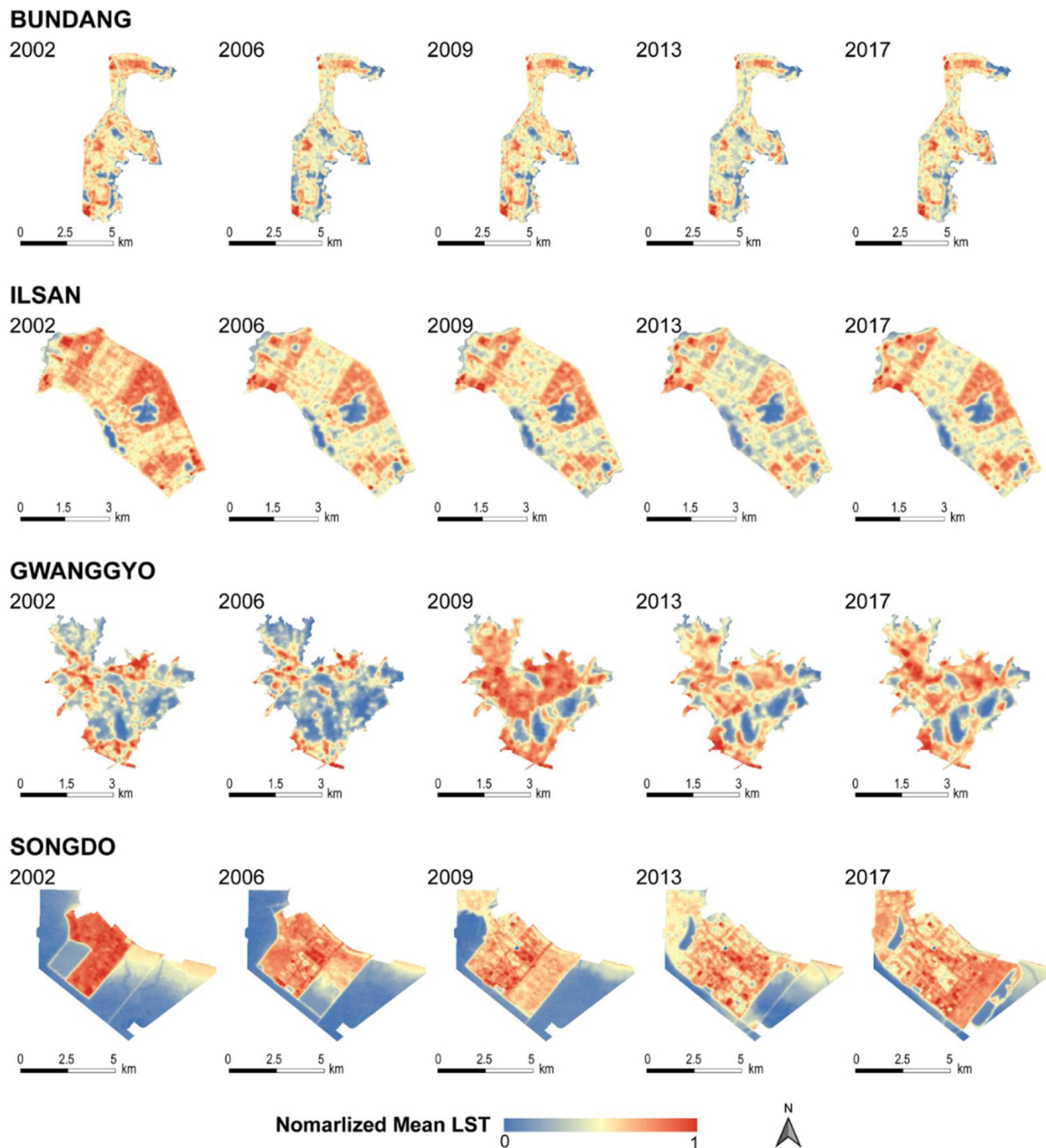


Fig. 3. Normalized changes in LST from 2002 to 2017 for each of our 4 study areas. Warmer colors indicate a higher LST.

towns (Bundang and Ilsan) is much smaller than that in the ‘recent’ towns (Gwanggyo and Songdo). Furthermore, Cluster 3 of Ilsan presents the highest mean LST value (30.32 °C) with the largest proportion, whereas Songdo has the lowest LST values in both Cluster 1 (23.26 °C) and Cluster 3 (29.88 °C) with the largest proportion of Cluster 1 (21.15 %).

Fig. 5 illustrates the trajectories of LST for the three clusters of each city, depicting the temporal thermal dynamics over the study period. In the same way of averaging the 2017 datasets, the yearly mean datasets were created and standardized by their standard deviations in order to adjust any outlier value possibly derived from anomalous atmospheric conditions or instrument malfunction. Between the three clusters, Cluster 3 generally exhibits an increase in the standardized mean LST (SLST) for all study areas. The increasing SLST of Cluster 3 may result from the combination of several reasons, including global warming and

urbanization. However, we report that the SLST of Cluster 3 markedly increases only in the ‘recent’ new towns where aggressive urbanization took place during the study period. These increases seem much significant when compared with the trajectories of SLST of Cluster 3 shown in the ‘old’ new towns where any significant development or environmental change did not occur over the period. Especially, SLST of Cluster 3 in Songdo presents the most dramatic change between 2009 and 2017, arguably because the Cluster 3 areas mostly consist of the reclaimed lands and include the major construction sites (the Incheon New Port and the Incheon Global Campus). On the flip side, SLST of Cluster 1, which mostly represents the temperature of green and blue spaces, show significant decreases in both Gwanggyo and Songdo. These decreases are attributed to the drastic increases in SLST of Cluster 3 pertaining to the dramatic urbanization, as SLST keeps a mean value of zero.

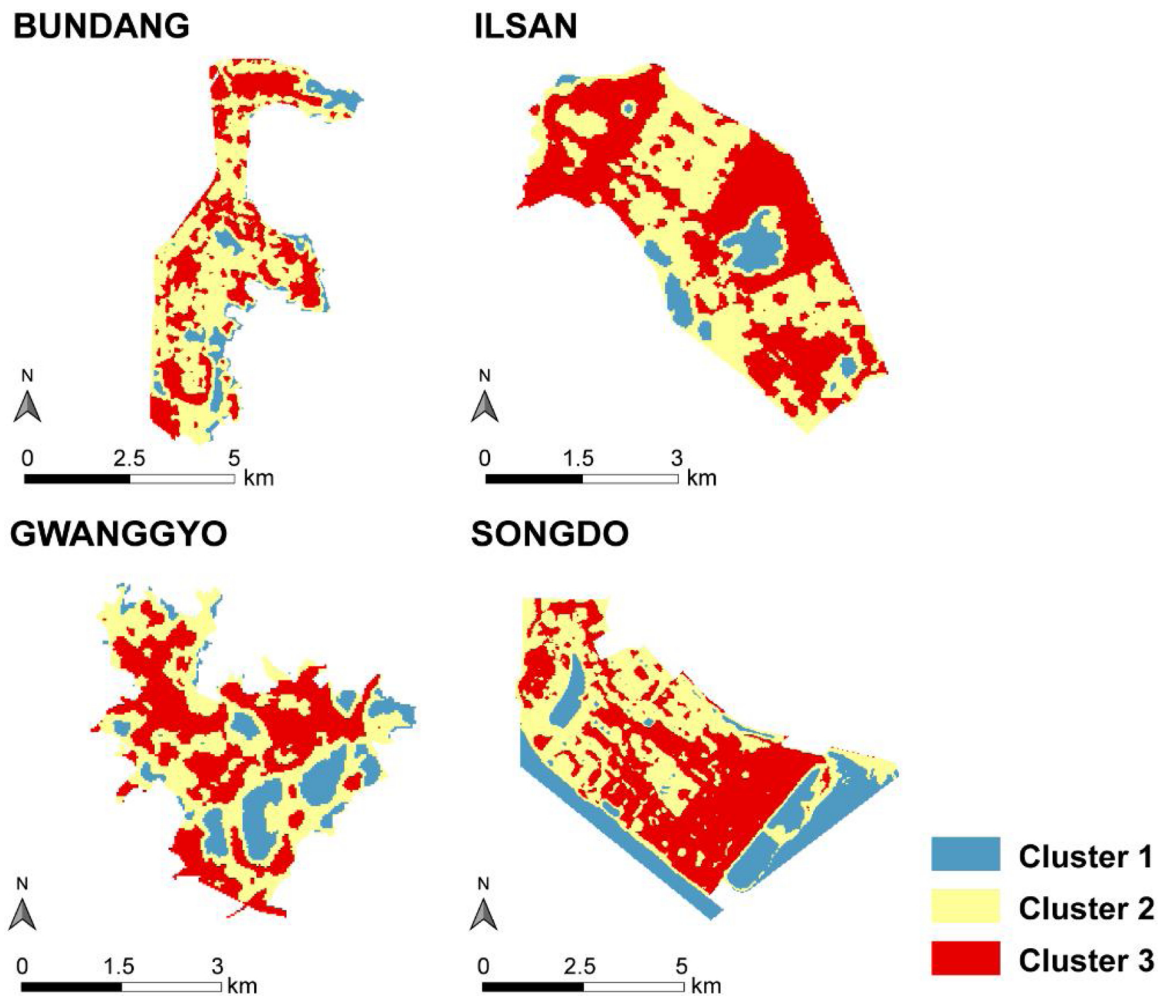


Fig. 4. Clustering results (3 levels – red, blue, and yellow) for our 4 study areas: Bundang, Ilsan, Gwanggyo, and Songdo.

Table 3
Descriptive statistics for the three clusters. Factors are from the average of the four 2017 datasets that cover all study areas.

	Clusters	Area (%)	Min. LST (°C)	Max. LST (°C)	Mean LST (°C)	Std. Dev.
Bundang	Cluster 1	9.02	22.33	25.73	24.62	0.73
	Cluster 2	55.23	25.73	28.87	27.71	0.78
	Cluster 3	35.75	28.87	38.45	29.98	1.06
Ilsan	Cluster 1	6.20	23.01	25.73	24.51	0.73
	Cluster 2	44.54	25.73	28.87	27.86	0.72
	Cluster 3	49.27	28.87	37.13	30.32	1.05
Gwanggyo	Cluster 1	16.27	22.69	25.73	24.54	0.79
	Cluster 2	43.16	25.73	28.87	27.60	0.89
	Cluster 3	40.56	28.87	34.63	30.07	0.91
Songdo	Cluster 1	21.15	19.34	25.73	23.26	1.46
	Cluster 2	38.60	25.73	28.87	27.63	0.86
	Cluster 3	40.24	28.87	37.26	29.88	0.79

The results show an incremental gap in temperatures between Cluster 1 and Cluster 3 – the low and the high cluster. Based on our hypothesis on the relationship between UHI and urbanization, for each study area, Cluster 3 s should represent the most urbanized areas and Cluster 1 s should represent the least.

We use frequency of perviousness as a proxy for urbanized intensities. Fig. 6 Frequency of impervious surface for each cluster of each city describes the results of our perviousness frequency analysis for each cluster in each study area. For every study area, Cluster 3 s have the largest frequency of perviousness (approximately 0.9) while Cluster

1 s represent the smallest frequency of perviousness (smaller than 0.1). The mean LST is also highest in Cluster 3 s and lowest in Cluster 1 s for every study area (Table 3 and Fig. 5). This helps confirm that Cluster 3 s represent the intensely urbanized areas, followed by Cluster 2 (moderately urbanized area), and Cluster 1 (the least urbanized area).

Two notable differences were found between the ‘old’ new towns and the ‘recent’ new towns (Figs. 5 and 6). First, changes in LST in both Bundang and Ilsan are minimal and the gaps between Cluster 1 and Cluster 3 remain large and relatively stable over our study time period. Second, imperviousness frequencies in Cluster 2 s for Bundang and Ilsan area are higher than the ‘recent’ new towns (Gwanggyo and Songdo).

5.2. Landscape and sociocultural factors

Results of our best-fit models that describe the relations between the six urban factors and LST for the study areas are shown in Table 4. (see <http://leam.illinois.edu/UHI/SUPPLEMENTARY.html> for visualizations of the six factors for each study town (24 maps)). We compared AIC values for linear and quadratic models and determined the best fit model for each variable. Cubic and quartic models were excluded because the overfitting can distort the interpretation. The explanatory variables were normalized between 0 and 1 to enable a comparison between different types of variables across the study areas. The significant relations vary from city to city, indicating differences in landscape or sociocultural conditions. For every study area, both vegetation (GNDVI) and impervious surfaces (NDBI) are found to have a significant influence on LST, explaining over 80 % of the variation. This is in-line

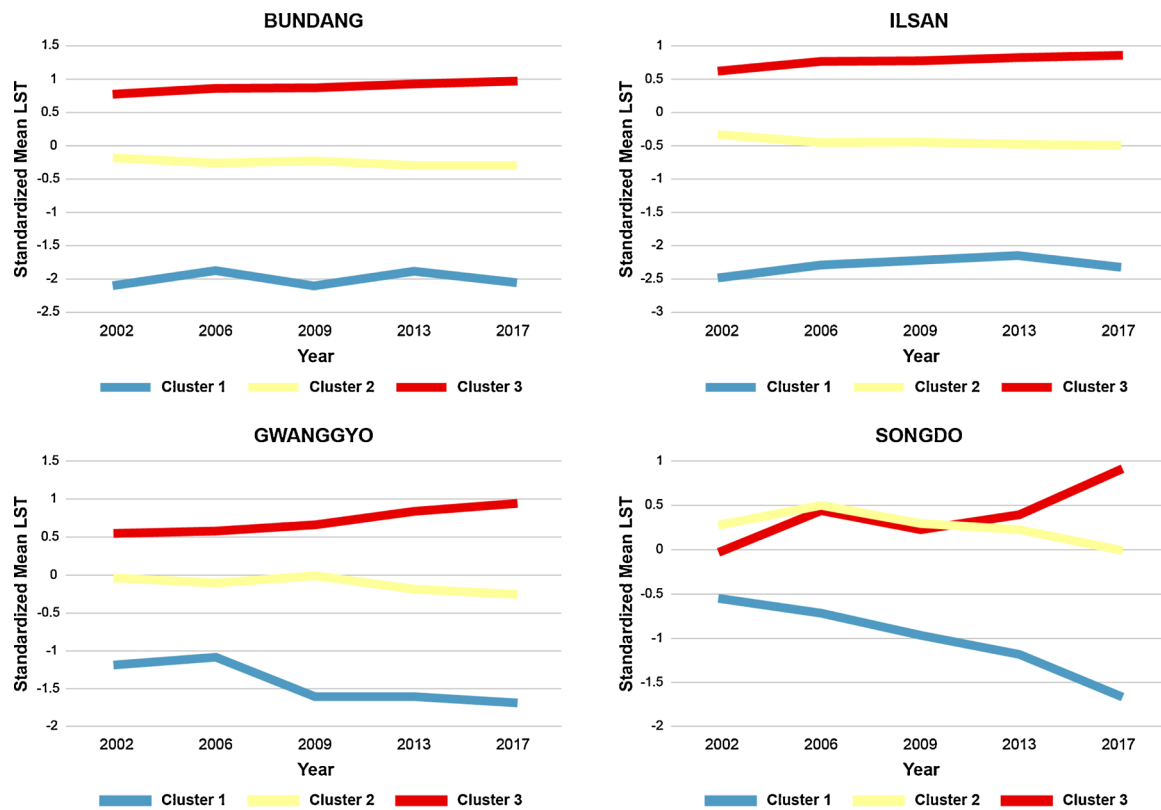


Fig. 5. Trajectories of LST of the clusters over the study period for each study city. LST values were standardized by their standard deviation to adjust outlier, having a mean of zero for each year and city.

with the previous literature on the variables (Estoque & Murayama, 2017; Tran et al., 2006). The presence of water appears to be significantly associated with LST ($p < 0.001$) in the towns where a relatively large water body is situated. More specifically, Songdo (a coastal city) presents the highest explanatory power of MNDWI to LST ($R^2 = 0.90$), followed by Gwanggyo (having two large lakes; $R^2 = 0.58$), Ilsan (having one lake; $R^2 = 0.38$). DEM is associated with LST in Bundang and Gwanggyo ($p < 0.001$) which have hilly topography, and in Songdo ($p < 0.01$) where the reclaimed lands must be higher than sea level. EDR shows statistical significance ($p < 0.01$) only in the ‘recent’ new towns, while PD shows a relation, at a significance level of 0.05, only in the ‘old’ ones where the high population density is one of the distinctive characteristics.

A visualization of our best mapping relations between the six urban factors (GNDVI, MDNWI, DEM, NDBI, and EDR) and LST for the study towns is shown in Fig. 7. The horizontal axis of each graph represents the normalized values of the six factors, and the vertical axis displays the expected LST ($^{\circ}\text{C}$) for areas within a certain parameter range.

Each town shows a similarly decreasing pattern of LST related to GDNVI and an increasing pattern related to NDBI. These polar patterns are understandable, given that as the abundance of vegetation increases, the built-up ratio decreases generally. About the normalized GDNVI, we note that the first derivative of the curve appears positive for the values approximately less than 0.2 since the value of 0 indicates non-vegetated areas, including water. Both GNDVI and NDBI in Songdo are best fitted using a cubic curve, and these patterns might be attributed to the anomalous heat from construction sites (heat from partially built-up areas) in 2017. Except for the low values of the normalized GDNVI, the relations between GDNVI and LST virtually seem to be negative linear relationships, whereas the relations between NDBI and LST are close to the positive linear ones.

MNDWI represents the presence of the water body within the study area, and LST significantly decreases as cells move closer to water.

Since low values of the normalized MNDWI represent non-water areas including built-up and vegetated areas, most of the data points aggregate close to 0, while only the small number appear at higher values (> 0.5) which indicate a lake in Ilsan, two lakes in Gwanggyo, the sea in Songdo. However, the results obviously display the low LST values for the cells corresponding to water, and this might suggest that water bodies in the towns exert a strong cooling effect. In comparison with the normalized GNDVI at the same values, the results additionally suggest that MNDVI has a more significant effect on lowering LST.

As previous studies showed different relations (either positive or negative) between LST and elevation (Khandelwal et al., 2018; Mathew et al., 2018; Phan et al., 2018), our results also show different ones across the cities. While a negative linear relation is shown in Bundang, the expected LST demonstrates a linearly increasing pattern in both Gwanggyo and Songdo. Therefore, we interpret DEM as an indirect indicator of UHI that represents the geographical distribution of the biophysical characteristics. For example, the most probable explanation for the positive linear relation in Songdo is that sea level is lower than the reclaimed, urbanized land. Details are discussed in the next section.

The normalized EDR is negatively and linearly related to LST in Gwanggyo, while Songdo exhibits a polynomial curve with a decreasing pattern for the value approximately less than 0.3 and an increasing pattern after 0.3. The negative relations are understandable considering the heat from major roads as well as the low proximity to natural areas (green and blue spaces) from major roads. The increasing pattern observed in Songdo may derive from the large construction sites because they are located far from major roads, at the periphery of the city – the northern and southern parts.

6. Discussion

Our spatiotemporal analyses of LST explicitly reveals differences in urbanization patterns and processes across the study areas. Clustering

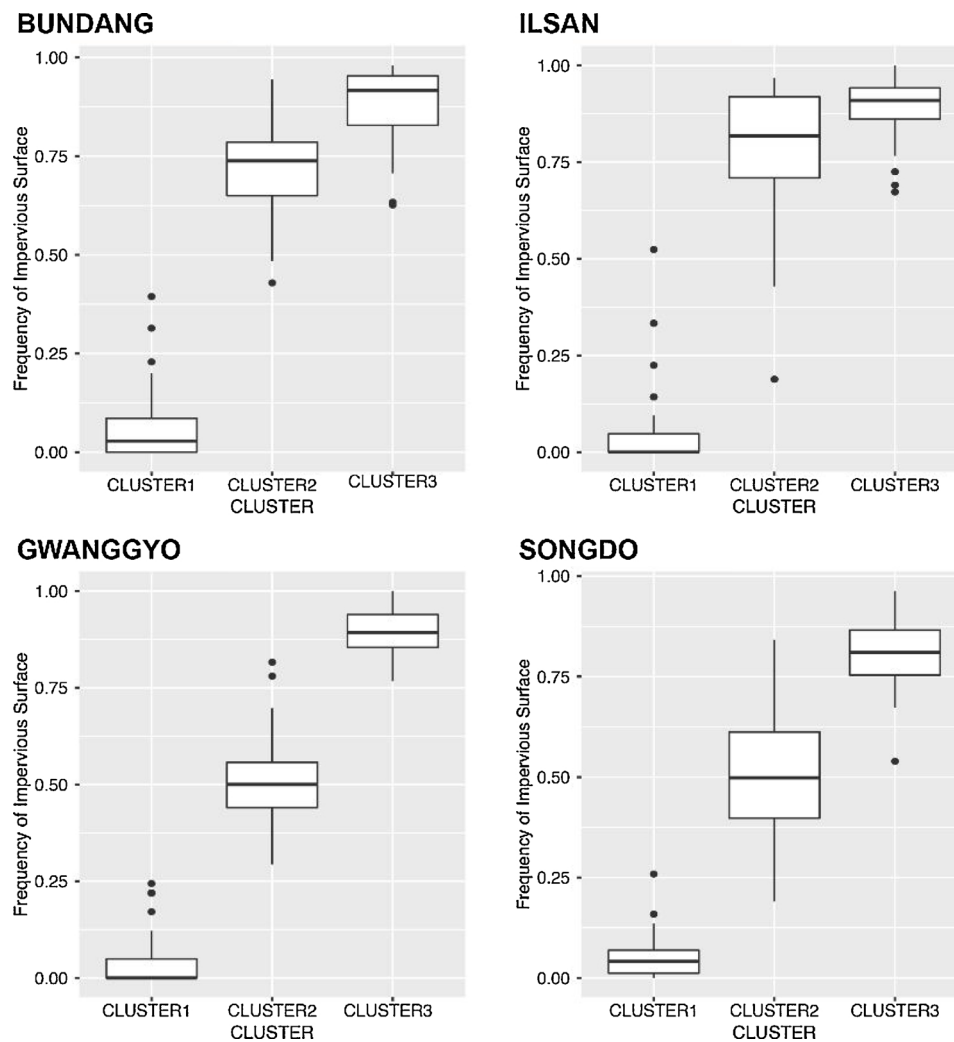


Fig. 6. Frequency of impervious surface for each cluster of each city. The frequency of impervious surface was calculated by assigning 1 to the 30 m grid cells of impervious surfaces and 0 to the cells of pervious surfaces.

the LST values also help classify the study areas by these urbanization differences.

Our results in Gwanggyo and Songdo indicate that the UHI phenomenon can be explicitly tracked during their respective urbanization processes over the study period. We further found that the gap in LST between the most urbanized area (Cluster 3) and the least urbanized area (Cluster 1) increases in the ‘recent’ new towns. This is in agreement with the findings of previous studies that demonstrate a positive relation between LST and the intensity of urbanization (Mathew et al., 2018; Sheng et al., 2017; Tran et al., 2006).

We also observe that the thermal gap between the contrasting clusters remained consistently large in the ‘old’ new towns – not unexpected since urbanization had been fully processed before the study period in each. The UHIs in those towns were seemingly ‘stable’ around the large gap in clusters. This implies that those towns were already experiencing aggravated UHIs. We might infer from this that in our ‘recent’ new towns, the thermal gap between Cluster 1 and Cluster 3 will continue to increase until they stabilize around a large gap, similar to his ‘old’ observation – unless interventions like appropriate UHI regulations or guidelines for further development are enacted.

However, we emphasize that the LST trends shown in Fig. 5 do not directly indicate the absolute UHI intensity. They instead illustrate the process of UHI formation in response to urbanization. In other words, although we observed that the LST gap between Cluster 1 and Cluster 3 in the ‘recent’ new towns continued to increase dramatically, we cannot

simply conclude that those towns confronted more aggravated UHI than the ‘old’ new towns. Based on our findings, we argue that the absolute intensity, which is doubtless affected by how UHI has been considered and managed, is tied closely to the proportion of the least urbanized areas (Cluster 1; Table 3) and the frequency of impervious surface (Fig. 6). Both the proportion and the frequency exhibited pronounced differences in the values between the ‘old’ new towns and the ‘recent’ ones.

In this paper, we have emphasized the fact that the emergence of urban sustainability in the 1990s greatly affected Korea city planning with respect to urban forms and structures. Gwanggyo and Songdo are the representative beneficiaries of the cutting-edge concepts, while those concepts were barely considered for planning Bundang and Ilsan. Our findings showed the higher proportion of Cluster 1 and the lower impervious surfaces frequency in Cluster 2 in the ‘recent’ new towns, and these differences may describe the larger capacity of the towns to withstand the influence of urbanization on temperature. On the other hand, we also found that the UHI phenomenon was continuously exacerbated for the last 15 years in the ‘recent’ new towns as they were urbanized dramatically. Therefore, albeit the applications of sustainability planning, we assert the need for robust UHI management regulations for those towns in order to avoid such ‘stabilized’ adverse conditions found in the ‘old’ new towns.

Table 4
Best models (lowest AIC) for the six factors for the study areas.

Study area	Variable	Best Model	R ²
Bundang	GNDVI***	y = 28.87 + 3.56 x - 8.59x ²	0.96
	MNDWI	y = 28.29 - 2.77x	0.03
	DEM***	y = 28.62 - 2x	0.32
	NDBI***	y = 23.06 + 19.28 x - 14.54x ²	0.95
	EDR*	y = 28.37 - 0.91x	0.06
	PD*	y = 27.96 + 3.78 x - 5.83x ²	0.09
Ilsan	GNDVI***	y = 28.2 + 7.89 x - 12.6x ²	0.78
	MNDWI***	y = 28.74 - 6.24x	0.38
	DEM	y = 28.75 - 0.80x	0.07
	NDBI***	y = 20.07 + 26.67 x - 18.17x ²	0.98
	EDR*	y = 28.73 + 0.44 x - 2.67x ²	0.12
	PD*	y = 28.38 + 4.35 x - 7.6x ²	0.14
Gwanggyo	GNDVI***	y = 26.06 + 15.87 x - 19.14x ²	0.90
	MNDWI***	y = 28.31 - 5.44x	0.58
	DEM**	y = 27.64 + 1.48x	0.11
	NDBI***	y = 23.12 + 14.93 x - 9.18x ²	0.97
	EDR**	y = 28.36 - 1.49x	0.13
	PD	y = 28.12 - 0.17x	0.03
Songdo	GNDVI***	y = 24.08 + 24.73 x - 27.94x ²	0.84
	MNDWI***	y = 28.68 - 16.08 x + 10.14x ²	0.90
	DEM**	y = 27.25 + 3.51x	0.15
	NDBI***	y = 10.69 + 48.65 x - 32.28x ²	0.96
	EDR***	y = 28.2 - 9.14 x + 13.86x ²	0.65
	PD	y = 27.58 + 2.34x	0.01

* p < .05.
** p < .01.
*** p < .001.

6.1. Different effects on LST across study areas

Fig. 7 shows that built-up areas (NDBI) play a major role in UHI in every test town, whereas both vegetation (GNDVI) and water (MNDWI) are significantly and negatively related to the rise of LST. With water, we found that its explanatory power was proportional to the amount within each city—Songdo showed the highest R² value, followed by Gwanggyo and Ilsan. This clearly indicates the significant cooling effect of water. The more amount of water a town (city) has, the better improvement we may expect in the thermal environment. Sensible monitoring of blue spaces can play a key role in UHI mitigation. This suggests the necessity of combined management strategies of both blue and green spaces (naturally or artificially) built in towns.

High population density is one of the major characteristics that can differentiate the ‘old’ new towns from the ‘recent’ ones. Our results (Table 4) represented this by showing a significant relation only in Bundang and Ilsan. Even with their low explanatory powers (R² values were smaller than 0.15 in both cities), the results demonstrate that if the density reaches a certain level, it can act as a driver of the UHI phenomenon. Yet, we also found that the density does not directly drive the rise of LST as it was best fitted using a polynomial curve in both towns (Fig. 8). From this, we assert that the population density is indirectly related to LST and the relation more likely depicts the distribution of housing. In both Bundang and Ilsan, normalized population density values are agglomerated close to low values (<0.2). Logically this suggests that most housings in the area are situated in unvegetated areas at low densities. After the values reached approximately 0.35, however, the expected LST decrease as PD increase, which may account for several luxurious housing complexes located around mountains or near green spaces in the towns.

We also found that elevation (DEM) and distance to roads (EDR) are indirectly related to UHI. Rather than directly explaining how they drive the rise of LST, these factors may indicate the spatial distribution of urban settings such as construction sites or vegetated areas. The negative relation between DEM and LST in Bundang indicates the

spatial distribution of small mountains or hills where the majority of them are used as neighborhood nature parks. These contrasting results regarding the effects of elevation were also reported in previous studies (Khandelwal et al., 2018; Mathew et al., 2018; Phan et al., 2018). In contrast to Bundang, both Gwanggyo and Songdo showed positive linear relationships. The most probable explanation in the case of Songdo is that sea level should be lower than the reclaimed, urbanized land. The result for Gwanggyo may represent its distinct geological dispersion of land-uses where many apartments are constructed on the mountain areas, and the two artificial lakes in the southern parts are made at a lower level. The relation between the normalized EDR and LST for Gwanggyo was negative. This is understandable considering the general low proximity of natural areas (green and blue spaces) to major roads. However, in Songdo, the curve was concave up, describing a positive trend for the values over 0.4 which would represent the construction sites (low accessibility and high temperature).

7. Conclusions

Understanding the driving forces of different UHIs helps planners, researchers, and decision-makers operationalize resilient development that allows cities to grow sensibly (within the limitations of a changing climate). And, UHIs are closely associated with achieving the sustainability at a city (or town) scale. As noted, it is undoubtable that monitoring UHIs and managing urbanization help improve public health and energy efficiency as well as control energy balance across a city. However, existing UHI studies reveal discrepancies in scales, methods, and results, which do not adequately capture the complexity of the phenomenon that induces different interactions with various components of urban environments (Cui et al., 2016). This may lead to a question regarding the reliability of the global or national UHI scaled studies when we adopt them to smaller-scale sustainability planning problems. In this paper, we analyzed four Korean new towns with different urban settings in order to identify how thermal dynamics illustrate the process of urbanization. Then we compared their statistical differences in order to reveal how some urban factors work differently across the study areas and to test the efficacy of sustainability policies. This comparative analysis helped discern the success of the development policies with a focus on the management of the UHIs. Controlling for climate conditions, we have verified our two hypotheses: 1) the spatiotemporal trajectories of LST exhibit the distinct pattern of urbanization of each town, and 2) the contributions of landscape and socio-cultural factors to the rise of LST are affected by the sustainability planning implemented in the study areas.

The success of sustainability planning cannot be simply determined by examining the UHIs however. A variety of investigations on social, environmental, and economic issues need to be carried out. Using comparative analysis, this research reveals that sustainable development policies have a notable effect on the patterns and intensities of UHI. Urban structures, planned under development policies, including green and blue space ratios, road networks, and housing distributions, were found to affect UHI significantly.

This work suggests that achieving urban sustainability requires understanding both landscape and socio-cultural complexities relating to UHI in order to understand past, current, and future states, improve the ability to overcome state changes, and develop planning strategies for governing with an eye toward environmental consequences. Important findings of this research include that the ‘recent’ new town currently confronts less aggressive UHI than the ‘old’ new towns, but the phenomenon has been dramatically exacerbated in recent years, necessitating continuous monitoring and improved (additional) mitigation strategies. We also found that the cooling effect of (larger scaled) water bodies is more effective than vegetation. This would suggest a new approach toward sustainability in Korean city planning - where greening has been generally regarded as a major solution for most of the urban UHI issues (KRIHS, 2000; Yoon, Kim, & Yeom, 2013).

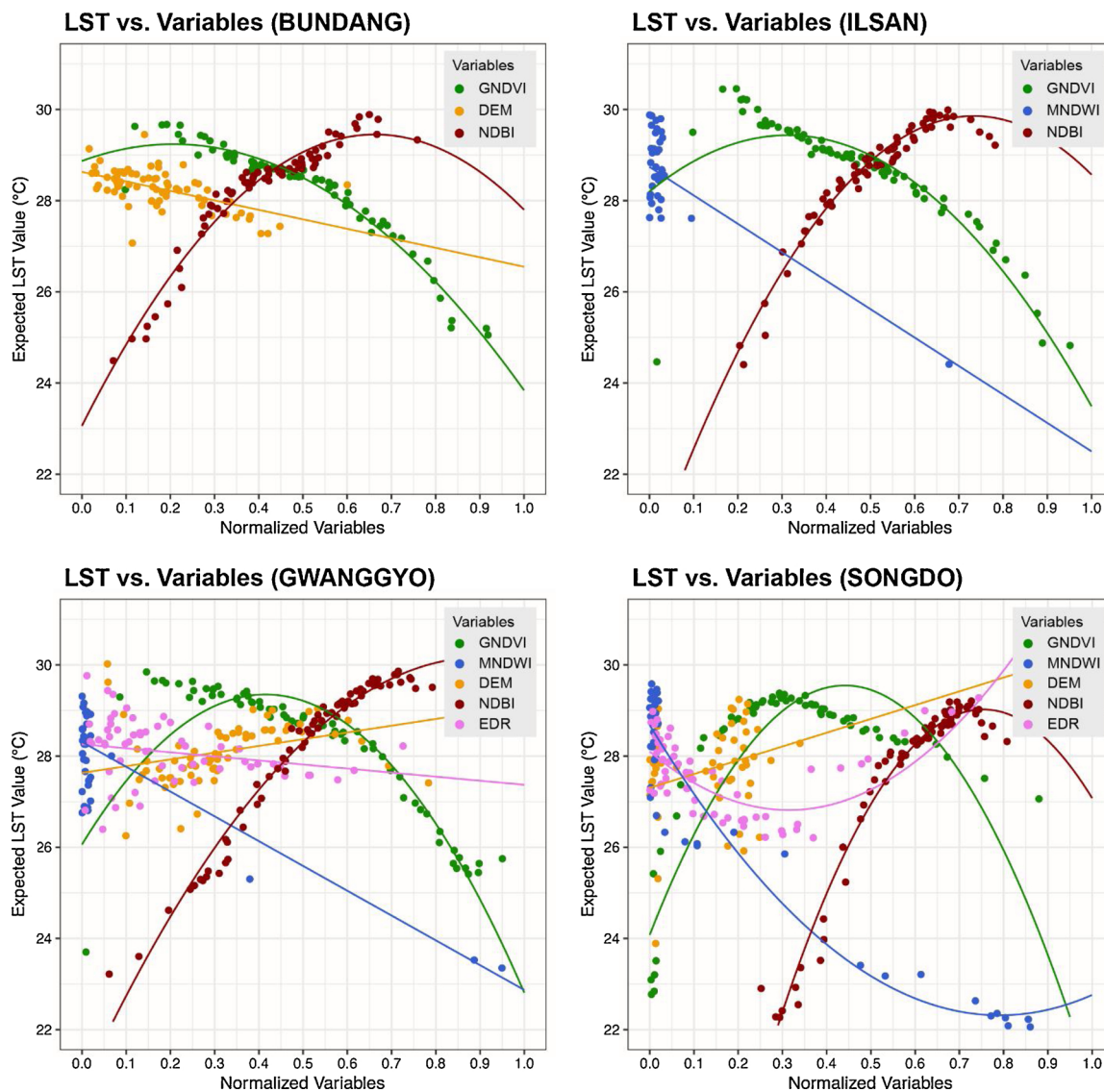


Fig. 7. Best mapping relations between LST and the selected variables ($p < 0.01$) for the study cities. GNDVI refers to the vegetation abundance, MDNWI refers to the water presence, DEM refers to the elevation, NDBI refers to the distribution of built-up area, and EDR refers to Euclidean distance to roads. The horizontal axis is the normalized values of the six factors, and the vertical axis displays the expected LST (°C) for areas within a certain parameter range.

In order to make our findings more valuable and useful, further points should be taken into consideration. First, we believe that the results will become more valid in assessing sustainability after Gwanggyo and Songdo are fully developed. The two areas in Songdo under construction in 2017 generated several biased results. Second,

additional analysis of new towns or cities in Korea under the same climate condition may be needed to support our claims more. Comparative analysis between the first five ‘old’ new towns (built before the mid-1990s) and the twelve ‘recent’ new towns (planned after the 2000s) will undoubtedly contribute to efforts to move from

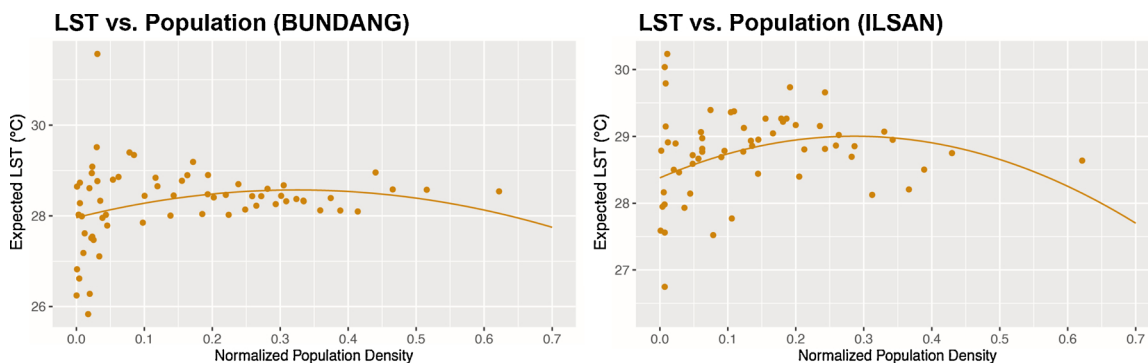


Fig. 8. Relation between normalized population density and Expected LST ($p < 0.05$) in Bundang (left) and Ilsan (right).

traditional city development to the robust and sustainable development that takes into account the thermal environment and urbanization conditions. Lastly, since the negative values of the remote sensing factors, such as GDNVI, were problematic, alternative factors such as the density of vegetation (Ashcroft, Gollan, & Ramp, 2014) should be considered.

This comparative research examined how sustainability planning affected context-dependent UHI. It quantified the relations between UHI and factors of influence through the combination of machine learning and statistical methods. We quantifiably illustrated the urban thermal dynamics of the four new towns in Korea and confirmed that the sustainability policies implemented in planning the 'recent' new towns allowed the towns to experience less aggravated UHIs than the 'old' new towns. However, at the same time, the increasing LST gap between the contrasting urban clusters found in the 'recent' new towns indicates a need to develop appropriate, long-term UHI management regulations. This paper provides a solid basis for improving Korean new town planning and managing the environmental issues in urban systems for planners, designers, and decision-makers to establish the sustainable built environment.

Declaration of Competing Interest

The submitted work is our own and that copyright has not been breached in seeking its publication. The submitted work has not previously been published in full and is not being considered for publication elsewhere.

Acknowledgments

This work was conducted with the support of the Korea Environment Industry & Technology Institute (KEITI) through its Urban Ecological Health Promotion Technology Development Project, and funded by the Korea Ministry of Environment (MOE) (2019002760001)

References

- Arifwidodo, S., & Chandrasiri, O. (2015). Urban heat island and household energy consumption in Bangkok, Thailand. *Energy Procedia*, 79, 189–194. <https://doi.org/10.1016/J.EGYPRO.2015.11.461>.
- Ashcroft, M. B., Gollan, J. R., & Ramp, D. (2014). Creating vegetation density profiles for a diverse range of ecological habitats using terrestrial laser scanning. *Methods in Ecology and Evolution*, 5(3), 263–272. <https://doi.org/10.1111/2041-210X.12157>.
- Bokaie, M., Zarkesh, M. K., Arasteh, P. D., & Hosseini, A. (2016). Assessment of Urban Heat Island based on the relationship between land surface temperature and Land Use/ Land Cover in Tehran. *Sustainable Cities and Society*, 23, 94–104. <https://doi.org/10.1016/J.SCS.2016.03.009>.
- Bozorgi, M., Nejadkoorki, F., & Mousavi, M. B. (2018). Land surface temperature estimating in urbanized landscapes using artificial neural networks. *Environmental Monitoring and Assessment*, 190(4), <https://doi.org/10.1007/s10661-018-6618-2>.
- Chun, B., & Guldmann, J.-M. (2014). Spatial statistical analysis and simulation of the urban heat island in high-density central cities. *Landscape and Urban Planning*, 125, 76–88. <https://doi.org/10.1016/J.LANDURBPLAN.2014.01.016>.
- Clinton, N., & Gong, P. (2013). MODIS detected surface urban heat islands and sinks: Global locations and controls. *Remote Sensing of Environment*, 134, 294–304. <https://doi.org/10.1016/J.RSE.2013.03.008>.
- Connors, J. P., Galletti, C. S., & Chow, W. T. L. (2013). Landscape configuration and urban heat island effects: Assessing the relationship between landscape characteristics and land surface temperature in Phoenix, Arizona. *Landscape Ecology*, 28(2), 271–283. <https://doi.org/10.1007/s10980-012-9833-1>.
- Coutts, A. M., Beringer, J., & Tapper, N. J. (2007). Impact of increasing urban density on local climate: Spatial and temporal variations in the surface energy balance in Melbourne, Australia. *Journal of Applied Meteorology and Climatology*, 46(4), 477–493. <https://doi.org/10.1175/JAM2462.1>.
- Cui, Y., Xu, X., Dong, J., & Qin, Y. (2016). Influence of urbanization factors on surface urban heat island intensity: A comparison of countries at different developmental phases. *Sustainability (Switzerland)*. <https://doi.org/10.3390/su8080706>.
- Eigenbrod, F., Bell, V. A., Davies, H. N., Heinemeyer, A., Armsworth, P. R., & Gaston, K. J. (2011). The impact of projected increases in urbanization on ecosystem services. *Proceedings Biological Sciences*, 278(1722), 3201–3208. <https://doi.org/10.1098/rspb.2010.2754>.
- Erell, E., & Williamson, T. (2006). Simulating air temperature in an urban street canyon in all weather conditions using measured data at a reference meteorological station. *International Journal of Climatology*, 26, 1671–1694. <https://doi.org/10.1002/joc.1328>.
- Esche, H. A., Franklin, S. E., & Wulder, M. A. (2002). Assessing cloud contamination effects on K-means unsupervised classifications of Landsat data. *Geoscience and Remote Sensing Symposium*, 2002. IGARSS'02. 2002. *IEEE International*, 6(C), 3387–3389. <https://doi.org/10.1109/IGARSS.2002.1027191>.
- Estoque, R. C., & Murayama, Y. (2017). Monitoring surface urban heat island formation in a tropical mountain city using Landsat data (1987–2015). *ISPRS Journal of Photogrammetry and Remote Sensing*, 133, 18–29. <https://doi.org/10.1016/j.isprsjprs.2017.09.008>.
- Estoque, R. C., Murayama, Y., & Myint, S. W. (2017). Effects of landscape composition and pattern on land surface temperature: An urban heat island study in the megacities of Southeast Asia. *The Science of the Total Environment*, 577, 349–359. <https://doi.org/10.1016/j.scitotenv.2016.10.195>.
- Feng, H., Zhao, X., Chen, F., & Wu, L. (2014). Using land use change trajectories to quantify the effects of urbanization on urban heat island. *Advances in Space Research*, 53(3), 463–473. <https://doi.org/10.1016/J.ASR.2013.11.028>.
- Founda, D., & Santamouris, M. (2017). Synergies between Urban Heat Island and Heat Waves in Athens (Greece), during an extremely hot summer (2012). *Scientific Reports*, 7(1), 10973. <https://doi.org/10.1038/s41598-017-11407-6>.
- Gitelson, A. A., Kaufman, Y. J., & Merzlyak, M. N. (1996). Use of a green channel in remote sensing of global vegetation from EOS-MODIS. *Remote Sensing of Environment*, 58(3), 289–298. [https://doi.org/10.1016/S0034-4257\(96\)00072-7](https://doi.org/10.1016/S0034-4257(96)00072-7).
- Golden, J. S. (2004). The built environment induced urban heat island effect in rapidly urbanizing arid regions – A sustainable urban engineering complexity. *Environmental Sciences*, 1(4), 321–349. <https://doi.org/10.1080/15693430412331291698>.
- Grimm, N. B., Faeth, S. H., Golubiewski, N. E., Redman, C. L., Wu, J., Bai, X., et al. (2008). Global change and the ecology of cities. *Science*, 319(5864), 756–760. <https://doi.org/10.1126/science.1150195>.
- Heaviside, C., Vardoulakis, S., & Cai, X.-M. (2016). Attribution of mortality to the urban heat island during heatwaves in the West Midlands, UK. *Environmental Health A Global Access Science Source*, 15(S1), S27. <https://doi.org/10.1186/s12940-016-0100-9>.
- Imhoff, M. L., Zhang, P., Wolfe, R. E., & Bounoua, L. (2010). Urban heat island effect across biomes in the continental USA. *International Geoscience and Remote Sensing Symposium (IGARSS)*, 114(3), 1920–1923. <https://doi.org/10.1109/IGARSS.2010.5653907>.
- Incheon Free Economic Zone (2018). *Incheon free economic zone*. Retrieved November 15, 2018, from <http://www.ifez.go.kr>.
- Ju, Y., Dronova, I., Ma, Q., & Zhang, X. (2017). Analysis of urbanization dynamics in mainland China using pixel-based night-time light trajectories from 1992 to 2013. *International Journal of Remote Sensing*, 38(21), 6047–6072. <https://doi.org/10.1080/01431161.2017.1302114>.
- Keeratikasikorn, C., Bonafoni, S., Keeratikasikorn, C., & Bonafoni, S. (2018). Satellite images and gaussian parameterization for an extensive analysis of urban heat islands in Thailand. *Remote Sensing*, 10(5), 665. <https://doi.org/10.3390/rs10050665>.
- Khandelwal, S., Goyal, R., Kaul, N., & Mathew, A. (2018). Assessment of land surface temperature variation due to change in elevation of area surrounding Jaipur, India. *The Egyptian Journal of Remote Sensing and Space Science*, 21(1), 87–94. <https://doi.org/10.1016/j.ejrs.2017.01.005>.
- Kim, Y., Jung, & Choi, M. J. (2018). Contracting-out public-private partnerships in mega-scale developments: The case of New Songdo City in Korea. *Cities*, 72(August 2017), 43–50. <https://doi.org/10.1016/j.cities.2017.07.021>.
- Kindu, M., Schneider, T., Teketay, D., & Knoke, T. (2013). Land Use/Land cover change analysis using object-based classification approach in munessa-shashemene landscape of the Ethiopian highlands. *Remote Sensing*, 5(5), 2411–2435. <https://doi.org/10.3390/rs5052411>.
- KMA (Korea Meteorological Administration) (2018). *Korea meteorological administration*. Retrieved December 8, 2018, from https://www.weather.go.kr/weather/climate/past_cal.jsp.
- Kolokotroni, M., & Giridharan, R. (2008). Urban heat island intensity in London: An investigation of the impact of physical characteristics on changes in outdoor air temperature during summer. *Solar Energy*, 82(11), 986–998. <https://doi.org/10.1016/j.solener.2008.05.004>.
- KRIHS (Korea Research Institute for Human Settlements) (2000). *Growth control and new town development in the capital region*. Retrieved from <https://core.ac.uk/download/pdf/51172472.pdf>.
- Li, H., Zhou, Y., Li, X., Meng, L., Wang, X., Wu, S., et al. (2018). A new method to quantify surface urban heat island intensity. *The Science of the Total Environment*, 624, 262–272. <https://doi.org/10.1016/j.scitotenv.2017.11.360>.
- Mahlkow, N., & Donner, J. (2017). From planning to implementation? The Role of climate change adaptation plans to tackle heat stress: A case study of Berlin, Germany. *Journal of Planning Education and Research*, 37(4), 385–396. <https://doi.org/10.1177/0739456X16664787>.
- Mathew, A., Khandelwal, S., & Kaul, N. (2016). Spatial and temporal variations of urban heat island effect and the effect of percentage impervious surface area and elevation on land surface temperature: Study of Chandigarh city, India. *Sustainable Cities and Society*, 26, 264–277. <https://doi.org/10.1016/j.scs.2016.06.018>.
- Mathew, A., Khandelwal, S., & Kaul, N. (2018). Investigating spatio-temporal surface urban heat island growth over Jaipur city using geospatial techniques. *Sustainable Cities and Society*, 40(April), 484–500. <https://doi.org/10.1016/j.scs.2018.04.018>.
- McFeeters, S. (1996). The use of the normalized difference water index (NDWI) in the delineation of open water features. *International Journal of Remote Sensing*, 17(7), 1425–1432. <https://doi.org/10.1080/01431169608948714>.
- Mehrotra, S., Bardhan, R., & Ramamritham, K. (2018). Urban informal housing and surface urban heat island intensity. *Environment and Urbanization Asia*, 9(2), 158–177. <https://doi.org/10.1177/0975425318783548>.

- MOLIT (Ministry of Land Infrastructure and Transport) (2017). *New towns concepts and construction status*. Retrieved October 6, 2018, from http://www.molit.go.kr/USR/policyData/m_34681/dtl.jsp?id=522.
- Mullins, P. D. (2017). The ubiquitous-eco-city of Songdo: An urban systems perspective on South Korea's green city approach. *Urban Planning*, 2(2), 4. <https://doi.org/10.17645/up.v2i2.933>.
- Pan, H., Deal, B., Chen, Y., & Hewings, G. (2018). A reassessment of urban structure and land-use patterns: Distance to CBD or network-based? — Evidence from Chicago. *Regional Science and Urban Economics*, 70, 215–228. <https://doi.org/10.1016/j.regsciurbeco.2018.04.009>.
- Peng, J., Xie, P., Liu, Y., & Ma, J. (2016). Urban thermal environment dynamics and associated landscape pattern factors: A case study in the Beijing metropolitan region. *Remote Sensing of Environment*, 173, 145–155. <https://doi.org/10.1016/j.rse.2015.11.027>.
- Phan, T., Kappas, M., Tran, T., Phan, T. N., Kappas, M., & Tran, T. P. (2018). Land surface temperature variation due to changes in elevation in Northwest Vietnam. *Climate*, 6(2), 28. <https://doi.org/10.3390/cli6020028>.
- Pickard, B. R., Van Berkel, D., Petrasova, A., & Meentemeyer, R. K. (2017). Forecasts of urbanization scenarios reveal trade-offs between landscape change and ecosystem services. *Landscape Ecology*, 32(3), 617–634. <https://doi.org/10.1007/s10980-016-0465-8>.
- Rasoolimanesh, S. M., Badaruzaman, N., & Jaafar, M. (2011). Achievement to sustainable urban development using city development strategies: A comparison between cities alliance and the World Bank definitions. *Journal of Sustainable Development*, 4(5), <https://doi.org/10.5539/jsd.v4n5p151>.
- Rousseeuw, P. J. (1987). Silhouettes: A graphical aid to the interpretation and validation of cluster analysis. *Journal of Computational and Applied Mathematics*, 20(C), 53–65. [https://doi.org/10.1016/0377-0427\(87\)90125-7](https://doi.org/10.1016/0377-0427(87)90125-7).
- Sagris, V., & Sepp, M. (2017). Landsat-8 TIRS data for assessing urban heat island effect and its impact on human health. *IEEE Geoscience and Remote Sensing Letters*, 14(12), 2385–2389. <https://doi.org/10.1109/LGRS.2017.2765703>.
- Shahraiyini, H. T., Soudoudi, S., El-Zafarany, A., El Seoud, T. A., Ashraf, H., & Krone, K. (2016). A comprehensive statistical study on daytime surface urban heat island during summer in urban areas, case study: Cairo and its new towns. *Remote Sensing*, 8(8), 1–20. <https://doi.org/10.3390/rs8080643>.
- Sheng, L., Tang, X., You, H., Gu, Q., & Hu, H. (2017). Comparison of the urban heat island intensity quantified by using air temperature and Landsat land surface temperature in Hangzhou, China. *Ecological Indicators*, 72, 738–746. <https://doi.org/10.1016/j.ecolind.2016.09.009>.
- Strahler, A. H. (1980). The use of prior probabilities in maximum likelihood classification of remotely sensed data. *Remote Sensing of Environment*, 10(2), 135–163. [https://doi.org/10.1016/0034-4257\(80\)90011-5](https://doi.org/10.1016/0034-4257(80)90011-5).
- Tibshirani, R., Walther, G., & Hastie, T. (2001). Estimating the number of clusters in a data set via the gap statistic. *Journal of the Royal Statistical Society. Series B: Statistical Methodology*, 63(2), 411–423. <https://doi.org/10.1111/1467-9868.00293>.
- Tran, H., Uchihama, D., Ochi, S., & Yasuoka, Y. (2006). Assessment with satellite data of the urban heat island effects in Asian mega cities. *International Journal of Applied Earth Observation and Geoinformation*, 8(1), 34–48. <https://doi.org/10.1016/j.jag.2005.05.003>.
- U.S. EPA (2008). *Urban heat Island basics. Reducing urban heat islands: Compendium of strategies*. Retrieved from <https://www.epa.gov/heat-islands/heat-island-compendium>.
- United Nations (2018). *The 2018 revision of world urbanization prospects*. Retrieved August 31, 2019, from <https://population.un.org/wup/>.
- Voelkel, J., & Shandas, V. (2017). Towards systematic prediction of urban heat islands: Grounding measurements, assessing modeling techniques. *Climate*, 5(2), 41. <https://doi.org/10.3390/cli5020041>.
- Voogt, J., & Oke, T. (2003). Thermal remote sensing of urban climates. *Remote Sensing of Environment*, 86(3), 370–384. [https://doi.org/10.1016/S0034-4257\(03\)00079-8](https://doi.org/10.1016/S0034-4257(03)00079-8).
- Wang, M., Abrams, Z. B., Kornblau, S. M., & Coombes, K. R. (2018). Thresher: Determining the number of clusters while removing outliers. *BMC Bioinformatics*, 19, 1–15. Retrieved from <http://10.0.4.162/s12859-017-1998-9>.
- Wang, S., Azzari, G., & Lobell, D. B. (2019). Crop type mapping without field-level labels: Random forest transfer and unsupervised clustering techniques. *Remote Sensing of Environment*, 222, 303–317. <https://doi.org/10.1016/j.rse.2018.12.026>.
- Weng, Q., Lu, D., & Schubring, J. (2004). Estimation of land surface temperature–vegetation abundance relationship for urban heat island studies. *Remote Sensing of Environment*, 89(4), 467–483. <https://doi.org/10.1016/j.rse.2003.11.005>.
- Xu, H. (2006). Modification of normalised difference water index (NDWI) to enhance open water features in remotely sensed imagery. *International Journal of Remote Sensing*, 27(14), 3025–3033. <https://doi.org/10.1080/01431160600589179>.
- Xu, H. (2010). Analysis of impervious surface and its impact on Urban heat environment using the normalized difference impervious surface index (NDISI). *Photogrammetric Engineering and Remote Sensing*, 76(5), 557–565. <https://doi.org/10.14358/PERS.76.5.557>.
- Yin, C., Yuan, M., Lu, Y., Huang, Y., & Liu, Y. (2018). Effects of urban form on the urban heat island effect based on spatial regression model. *The Science of the Total Environment*, 634, 696–704. <https://doi.org/10.1016/j.scitotenv.2018.03.350>.
- Yoon, E., Kim, H., & Yeom, J.-M. (2013). Analysis of Green Area changing in New-town 'Bundang': Focusing on LandsatTM Image analysis during the period 1985–2006. *Journal of Korea Planning Association*, 48(2), 329–340.
- Zha, Y., Gao, J., & Ni, S. (2003). Use of normalized difference built-up index in automatically mapping urban areas from TM imagery. *International Journal of Remote Sensing*, 24(3), 583–594. <https://doi.org/10.1080/01431160304987>.
- Zhao, L., Lee, X., Smith, R. B., & Oleson, K. (2014). Strong contributions of local background climate to urban heat islands. *Nature*, 511(7508), 216–219. <https://doi.org/10.1038/nature13462>.
- Zhou, D., Zhao, S., Liu, S., Zhang, L., & Zhu, C. (2014). Surface urban heat island in China's 32 major cities: Spatial patterns and drivers. *Remote Sensing of Environment*, 152, 51–61. <https://doi.org/10.1016/j.rse.2014.05.017>.
- Zhou, S., Xu, Z., & Liu, F. (2017). Method for determining the optimal number of clusters based on agglomerative hierarchical clustering. *IEEE Transactions on Neural Networks and Learning Systems*, 28(12), 3007–3017. Retrieved from <http://10.0.4.85/TNNLS.2016.2608001>.
- Zhu, R., Wong, M. S., Guilbert, É., & Chan, P.-W. (2017). Understanding heat patterns produced by vehicular flows in urban areas. *Scientific Reports*, 7(1), 16309. <https://doi.org/10.1038/s41598-017-15869-6>.